JACS
JOURNAL OF THE AMERICAN CHEMICAL SOCIETY
Article
pubs.acs.org/JACS

The Origin of Relative Intensity Fluctuations in Single-Molecule Tip-Enhanced Raman Spectroscopy

Matthew. D. Sonntag,[†] Dhabih Chulhai,[‡] Tamar Seideman,[†] Lasse Jensen,[‡] and Richard P. Van Duyne*[,†]

[†]Department of Chemistry, Northwestern University, Evanston, Illinois 60208, United States
[‡]Department of Chemistry, The Pennsylvania State University, University Park, Pennsylvania 16802, United States

Supporting Information

ABSTRACT: An explanation of the relative intensity fluctuations observed in single-molecule Raman experiments is described utilizing both single-molecule tip-enhanced Raman spectroscopy and time-dependent density functional theory calculations. No correlation is observed in mode to mode intensity fluctuations indicating that the changes in mode intensities are completely independent. Theoretical calculations provide convincing evidence that the fluctuations are not the result of diffusion, orientation, or local electromagnetic field gradients but rather are the result of subtle variations of the excited-state lifetime, energy, and geometry of the molecule. These variations in the excited-state properties will provide information on adsorbate−adsorbate and adsorbate−substrate interactions and may allow for inversion of experimental results to obtain these excited-state properties.

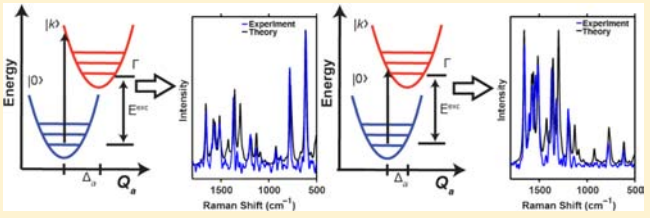

1. INTRODUCTION

In 1997, two independent reports observing single-molecule surface-enhanced Raman spectroscopy (SMSERS) contributed to a renaissance in SERS.[1,2] Nie and Emory reported the observation of SER spectra from single rhodamine 6G (R6G) molecules adsorbed on citrate-reduced Ag nanoparticles that were electrostatically immobilized on glass in an ambient environment. Strong intensity fluctuations occurred on the second time scale and were attributed to surface diffusion of molecules into and out of the electromagnetic enhancing hot spot.[3] Independently, Kneipp and co-workers observed SMSERS of crystal violet (CV) in citrate-reduced Ag nanoparticle aggregates in solution, the signal demonstrating a Poisson distribution of intensities corresponding to 0, 1, 2, or 3 molecules in the hot-spot.

Similarly, reports of single-molecule tip-enhanced Raman spectroscopy (SMTERS) have generated a tremendous amount of interest due to its ability to probe chemical information on the nanometer scale.[4−8] The combination of scanning tunneling microscopy (STM) with Raman spectroscopy can overcome the low sensitivity and diffraction limited spatial resolution associated with Raman spectroscopy as well as the limited chemical sensitivity associated with STM. TERS employs the use of a nanometallic tip to both localize and enhance the incident electric field.

After the initial SMSERS observations one of the major questions involved the nature of the sporadic intensity fluctuations (i.e., blinking), specifically what is their origin. There have been many reports studying blinking, demonstrating that the blinking dynamics are dependent on temperature,[3,9−11] excitation intensity,[12,13] and environment.[3,9,14] While the blinking dynamics have been demonstrated to be dependent on temperature, no changes in the relative intensities were observed during thermal heating of the sample during illumination.[3] Additionally, the fluctuations themselves have been treated with many models.[2,12,13,15−17]

In general, it appears that blinking is caused by diffusion of the molecule on the surface into and out of the hot spot. Previous work in both SMSERS and SMTERS utilized an isotopically edited extension of the bianalyte technique, which demonstrates strong evidence of a diffusion mechanism.[5,14] To date, multiple papers on SMSERS have focused on fluctuations both in peak intensity and spectral position, using statistical analysis to claim observance of single-molecule behavior. Within the TERS literature, similar fluctuations in intensity have also been used as a basis for identifying single-molecule behavior.[4,8] Fluctuations in the line shape and spectral position can also make characterization of samples difficult, as molecular decomposition and photobleaching are possible.[18,19]

Although dramatic changes in the Raman intensity and frequency of the Raman modes have been discussed at length (see above), more subtle changes are often evident in the Raman spectrum of single molecules. Large relative intensity fluctuations between individual modes within a single spectrum and changes in linewidths have been observed during the course of the experiment. There are several possible explanations for this behavior based on the properties of the molecule and the hot-spot itself. For example, in ambient conditions, a water meniscus forms in the tip−sample junction allowing the molecule to diffuse and sample different polarizations, orientations, enhancement factors, etc. This

Received: August 23, 2013
Published: September 30, 2013

© 2013 American Chemical Society

dx.doi.org/10.1021/ja408758j | J. Am. Chem. Soc. 2013, 135, 17187−17192

information may be used to gain some insight into the adsorbate−adsorbate and/or adsorbate−substrate interactions.

2. EXPERIMENTAL SECTION

Sample Preparation. The synthesis of R6G−d_0 is based on conditions given by Zhang[20] and has been reported elsewhere.[14] A standard solution (10^{-6} M in EtOH) of R6G−d_0 was created and analyzed by UV−vis absorbance spectroscopy to quantify concentration. The spectrophotometer consisted of a white light source (F−O Lite, World Precision Industries) fiber-coupled to a cuvette holder (CUV, Ocean Optics) with the output fiber-coupled to a visible light spectrometer (SD2000, Ocean Optics). Silver films (AgF) 200 nm thick were prepared by electron beam deposition (AXXIS, Kurt J. Lesker Co.) at a rate of 2 Å/s onto a glass coverslip. SMTERS samples were prepared by incubating the Ag films in a 1×10^{-6} M ethanolic solution of R6G−d_0 for at least 2 h. The samples were rinsed thoroughly with Milli-Q water and dried under N_2 prior to use.

Tip Preparation. The silver tips used in this experiment were prepared through electrochemical etching.[8] A 1:4 by volume mixture of perchloric acid (70%, Aldrich) and ethanol was used as the etching solution. A platinum ring with diameter 5 cm was used as the negative electrode. Silver wire (99.99%, Aldrich) with a diameter of 0.25 mm was employed as the positive electrode, and a constant voltage of 1.6 V was applied. The circuit was manually disconnected after the lower part of the wire dropped off. The tips were rinsed with water and ethanol after etching to remove any excess salts.

Instrumentation. Tip-enhanced spectra were collected on a home-built setup as described previously.[5] Briefly, a 532 nm laser (Spectra Physics Excelsior, 100 mW) was fiber-coupled to the optical microscope via a single-mode optical fiber. Excitation at 532 nm provides a resonant enhancement, and therefore, measurements are tip-enhanced resonance Raman spectroscopy (TERRS); however, in agreement with previous literature, we will refer to this as TERS. The laser light was passed through a filter to remove Raman light generated by the fiber (MaxLine laser line 532, Semrock) and polarizer to achieve the desired p polarization. The incident light was focused onto the tip−sample junction through an aspheric lens (f = 13.86 mm, NA = 0.18, Geltech Aspheric Lens) at an angle of 55° from the surface normal. Inelastic scattered light was collected through the same lens, filtered to remove residual laser light (RazorEdge long-pass 532, Semrock), and fiber-coupled to a spectrometer (IsoPlane SCT320, Princeton Instruments). The Raman light was dispersed by a 1200 groove/mm grating and collected on a thermoelectrically cooled CCD (PIXIS 400, Princeton Instruments). The tip approach and tunneling parameters were operated by a commercial STM system (Molecular Imaging) controlled by RHK electronics (SPM100). Experimental conditions for TERS experiments: λ_{ex} = 532 nm, power =0.4−0.6 mW, V = 300−500 mV, I = 3−5 nA.

Computational Modeling. The time-dependent wave packet formalism of the resonance Raman scattering (RRS) tensor (α), considering only the ground (G) and resonantly excited (E) state, may be written as[21]

$$\alpha_{\alpha\beta}^{p} = (\mu_{\alpha}^{GE})(\mu_{\beta}^{GE}) \times L[E^{EG}, \omega_p, \Delta_p, \Gamma] \quad (1)$$

where Greek subscripts refer to Cartesian directions, μ^{EG} is the transition dipole moment between the ground and resonantly excited state, L is a line shape function that depends on E^{EG} (the energy difference between G and E), ω_p (the frequency of the of vibrational mode p), Δ_p (the mode-dependent displacement between ground- and excited-state potential minima in ground-state dimensionless coordinates), and Γ (a spectral broadening parameter that is related to the lifetime of E). This equation also assumes the Condon approximation (no vibrational coordinate dependence on μ^{EG}). Within these approximations, the RRS spectrum may be simulated exactly providing that μ^{EG}, E^{EG}, ω_p, Δ_p, and Γ are known.

Simulations of the RRS of R6G were previously obtained using parameters calculated from a time-dependent density functional theory (TDDFT) method as outlined previously.[5] Geometry optimization, normal modes, and excited-state energy calculations were performed in NWChem[22] using the B3LYP/6-311G* level of theory. Vibrational frequencies were scaled by a factor of 0.98. Dimensionless displacements were obtained from a three-point numerical differentiation of excited state energies along mass weighted vibrational coordinates. The lifetime parameter was estimated from solution-phase R6G RRS experimental results and found to be ∼500 cm^{-1}. These parameters were shown to accurately simulate experimental ensemble RRS spectra of R6G.

In single-molecule observations, these parameters may vary reflecting the exact local environment of the molecule. To examine this possibility, we fitted simulated spectra using a least-squares method to experimental data allowing for small changes in the molecular parameters. Both experimental and simulated spectra were normalized (to the mode at ∼1658 cm^{-1}), and the least-squares minimization was performed using a multidimensional downhill simplex algorithm[23] allowing for variations in Δ_p, E^{EG}, and Γ. Calculated values (described above) were used as starting points in the simplex algorithm, with values of E^{EG} allowed to vary within ±25 nm of the initial value (532 nm) and Γ between 50−1500 cm^{-1}. The Δ_p of 10 selected modes were allowed to vary within ∼40% of their initial values. These modes (at p = 616, 772, 1195, 1298, 1356, 1515, 1561, 1579, 1607, and 1658 cm^{-1}) were selected because they were the largest contributors to the RRS spectrum in the region under examination (400−1800 cm^{-1}). The Δ_p of the remaining modes were kept fixed at their calculated values.

3. RESULTS AND DISCUSSION

Figure 1A shows a series of spectra collected continuously from the sample. Large frequency and intensity fluctuations of the signal are evident throughout the course of the acquisition, occurring on a time scale of several seconds. The blinking behavior (appearance and disappearance) occurs on a time scale of ∼30 s as shown in Figure 1A, thus the relative fluctuations are occurring on a time scale much faster than blinking. Figure 1B shows two representative spectra extracted from the waterfall plot in Figure 1A. Large changes in the relative peak intensities are readily apparent especially between the high and low energy portions of the spectra. The ratio of the integrated intensities of two modes (608:1651) changes from 3:1 in the blue curve to 1:5 in the red curve. These relative intensity changes occur on the time scale of several seconds. Additionally, the calculated Raman spectrum of rhodamine 6G is shown and corresponds well with the experimentally obtained data. Small shifts are observed between the experimental and theoretical vibrational frequencies (<10 cm^{-1}). The simulations were performed for an isolated molecule, neglecting solvent effects. Therefore, these discrepancies could be attributed to interactions between the molecules and the silver surface as well as intermolecular interactions.

Figure 2 shows in greater detail the intensity and frequency fluctuations focusing on four of the prominent vibrational modes present in the spectrum: those at 608, 771, 1362, and 1651 cm^{-1}. Figure 2A shows the change in integrated peak intensity as a function of time. Large changes in the total intensity of the modes are evident which is consistent with the diffusion mechanism of molecules entering and leaving the hot spot as discussed above. Closer examination of the traces of individual modes indicates that the integrated intensities rise and fall independent of one another. This indicates that that the changes are not due to diffusion of the molecules into and out of the highest enhancing region in the tip−sample junction. Figure 2B shows the time evolution of the spectral wandering for the four modes mentioned above. Changes in peak position of <7 cm^{-1} were observed, which is consistent with previous

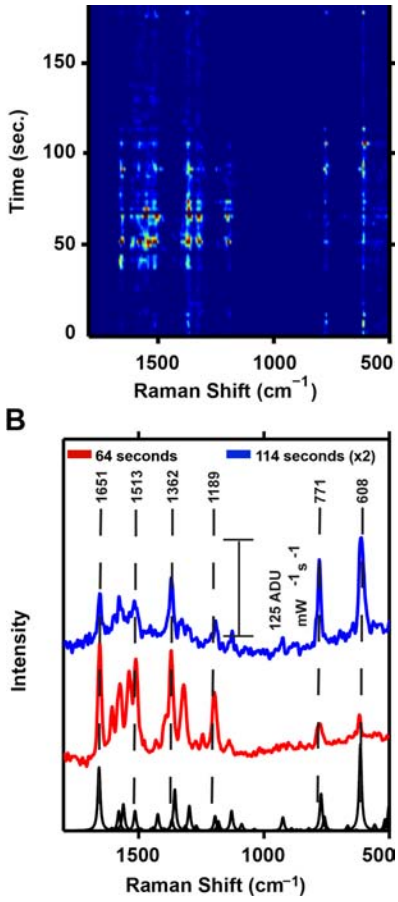

Figure 1. (A) Time series waterfall plot of spectra taken continuously with a single tip under single-molecule conditions. The false color represents signal intensity, where red is highest and blue is lowest. (B) Two representative spectra illustrating the large changes in relative intensity along with the theoretical spectrum. Spectra acquired with λ_{ex} = 532 nm, t_{aq} = 2 s, and I_{ex} = 520 μW and tunneling conditions of 3 nA and 500 mV.

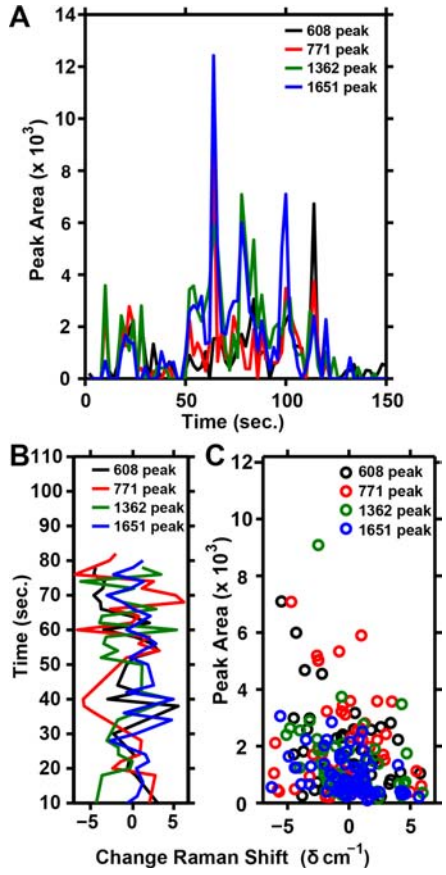

Figure 2. (A) Plot of the time evolution of the integrated peak intensity for four prominent vibrational modes in the spectrum. (B) Plot of the time evolution of the spectral wandering present in four different vibrational modes. (C) Plot of the relationship between the spectral wandering and the peak area of the four vibrational modes. Only data points with intensity greater than the limit of detection are shown. Spectra acquired with λ_{ex} = 532 nm, t_{aq} = 2 s, and I_{ex} = 520 μW and tunneling conditions of 3 nA and 500 mV.

reports.[5,14] One possible explanation for the observed changes in peak intensity is that shifts in the center frequency either enhance or damp the vibrational modes. If this were the case, then a relationship would exist between the spectral wandering and the peak; however, no such relationship exists for the four modes of interest as shown in Figure 2C.

Figure 3 illustrates the normal modes for the vibrational resonances examined in Figure 2. The majority of the vibrations are concentrated on the xanthene ring; however each mode contains slightly different normal mode character. It is possible that differing adsorption geometries could cause certain modes to be preferentially enhanced or damped. A more complete understanding of the relationship between different modes and the integrated intensities can be gained by examining the intensity changes across the entire experimental data set.

These changes in integrated peak intensity of the full data set can be examined via 2D correlation analysis.[24] If the modes are fluctuating in a truly independent fashion, then the time evolution of the four Raman modes should be noncorrelated ($\chi \approx 0$). One possible explanation for the relative intensity fluctuations is that the orientation or surface adsorption geometry of the molecules is damping certain vibrational resonances or enhancing others. If this is the case, the Raman modes in question should be anticorrelated ($\chi \approx -1$).

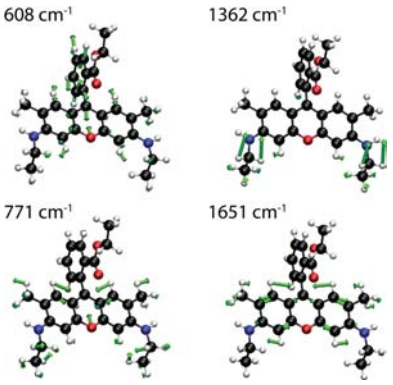

Figure 3. Visual depiction of the normal modes of the four most intense vibrations in the TERS spectrum of R6G.

Alternatively, if the intensities of two bands are changing together, then they will be correlated ($\chi \approx 1$). The cross correlation between two Raman shifts, i and j, is given by

$$\chi_{ij} = \frac{\sigma_{ij}}{\sqrt{\sigma_{ii}}\sqrt{\sigma_{jj}}} \quad (2)$$

where σ_{ij}, the covariance, is defined as

dx.doi.org/10.1021/ja408758j | J. Am. Chem. Soc. 2013, 135, 17187−17192

$$\sigma_{ij} = \sum_{t=0} [I(i, t) - \bar{I}(i)] \times [I(j, t) - \bar{I}(j)] \quad (3)$$

and $I(n,t)$ is the intensity of the Raman shift n at time t and $I(x)$ is the time-averaged intensity of the given Raman shift, n. The cross correlation, χ_{ij}, is calculated between all combinations of Raman shifts in the data set. This method only examines the zero time delay correlation but can be modified by introducing a delay factor into the above equation to examine any phase relationships that may exist in the data.

Figure 4 shows the covariance (A, σ_{ij}) and correlation (B, χ_{ij}) of the data collected in Figure 1A. In TERS as well as SERS,

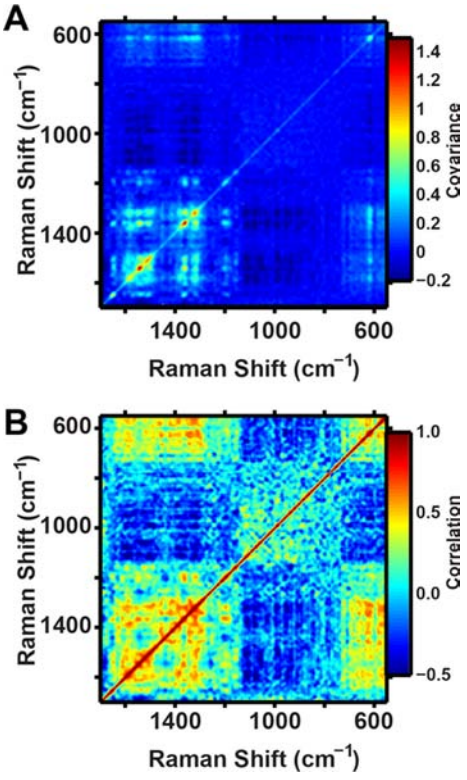

Figure 4. Zero time delay 2D (A) covariance and (B) cross-correlation of the time evolution data displayed in Figure 1.

there is a continuous background that covers the entire spectral region of interest and is especially pronounced around the vibrational modes. Moore et al. have demonstrated that a strong correlation exists between the Stokes bands and the continuum.[25] The spectra were normalized prior to analysis in an attempt to compensate for the changes in total intensity; however, this is difficult to remove as is evident by the slight correlation (χ = 0.2−0.4) present between all the vibrational modes. Additionally, the large changes in total intensity throughout the acquisition can cause some correlation between modes. There is no anticorrelation present between the modes in the spectrum, indicating that changes in the vibrational features are not inversely related. This noncorrelation of the data implies that the modes themselves are fluctuating in a truly independent fashion.

It has been shown that the orientation dependence of molecules with respect to the surface in SERS may be approximated using

$$I^{\mathrm{SERS}} \propto |\mathbf{E}_{\mathrm{loc}}(\omega_{\mathrm{L}}) \cdot \mathbf{R}^{T} \alpha \cdot \mathbf{R} \cdot \mathbf{E}_{\mathrm{loc}}(\omega_{\mathrm{S}})|^2$$

where $\mathbf{E}_{\mathrm{loc}}$ is the local field enhancement, α is the Raman tensor, and $\mathbf{R}$ is some rotation matrix.[7,26,27] This formalism can describe similar fluctuations observed in SMSERS experiments in which the relative intensities and peak positions are the result of molecular reorientation inside the hot spot.[26,28] However, this approximation cannot be used to correctly describe the relative mode intensities of the SERRS (TERRS) of a molecule resonantly excited to a single excited state, such as R6G. In such molecules, the resonance Raman tensor α (calculated using the time-dependent formalism presented in eq 1) depends on the line shape function L which is independent of rotation; orientation-dependence stems from rotation of a vector (the transition dipole) that, in the Condon approximation, is mode-independent.

While this results in orientation-independent relative intensities, the SERRS intensities calculated using the above equation will, however, result in largest enhancements for transition dipoles aligned with the local field vectors. Going beyond the Condon approximation, inclusion of the first Herzberg−Teller (B) term results in some orientation dependence of the SERRS spectrum for R6G, but its contribution is minor, with features that are 1−2 orders of magnitude weaker than the total intensity, and therefore is an unlikely explanation for the features observed in the SMTERS experiments. A similar argument could be made for field gradient effects since the electric dipole−quadrupole tensor contains the same line shape function. A more rigorous theoretical treatment would be required to account for fluctuations of individual modes in SERRS and TERRS. In particular, one would need to determine the orientation- and site-dependent coupling of the excited state (and therefore the properties that depend on this state, such as μ^{EG}, E^{EG}, Δ_{p}, and Γ) with the plasmonic surface.

Alternatively, one may be able to "invert" experimental data in order to obtain these excited-state properties.[29,30] Generic algorithms may be used to accurately obtain these parameters through nonlinear least-squares minimization, assuming that a good initial "guess" was first made. In this paper, we use the results of full TDDFT calculations as an initial "guess" in a multidimensional downhill simplex algorithm in order to obtain optimized parameters. Figure 5 shows the comparison between six frames of the experimental TERS and simulated RRS with optimized parameters of R6G. These frames were chosen because they show intense features at different regions in their

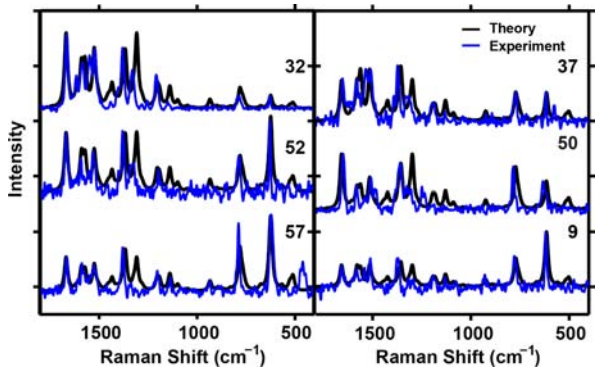

Figure 5. Plot of the experimental and theoretical spectra. The fluctuations can be reproduced by allowing for small changes in the properties of the excited state of the molecule. Different frames show certain regions of the spectrum dominating the total intensity.

dx.doi.org/10.1021/ja408758j | J. Am. Chem. Soc. 2013, 135, 17187−17192

Table 1. Parameters Used to Reproduce Experimental Spectra Obtained from Least-Squares Minimization of Excited-State Properties

parameter	calcd	09	32	37	50	52	57
Γ (cm^{-1})	–	545	1727	1159	654	601	489
E^{EG} (nm)	534	542	557	527	524	522	538
Δ_{616}	−0.245	−0.294	−0.164†	−0.205	−0.190†	−0.274	−0.274
Δ_{772}	−0.163	−0.181	−0.155	−0.166	−0.201	−0.157	−0.186
Δ_{1195}	−0.098	−0.089	−0.111	−0.089	−0.093	−0.101	−0.093
Δ_{1298}	−0.141	−0.151	−0.193†	−0.153	−0.196†	−0.176†	−0.160
Δ_{1356}	0.180	0.161	0.158	0.173	0.170	0.167	0.177
Δ_{1515}	−0.143	−0.162	−0.158	−0.169	−0.146	−0.146	−0.150
Δ_{1561}	0.145	0.140	0.130	0.158	0.117	0.130	0.126
Δ_{1579}	0.120	0.142	0.118	0.123	0.103	0.127	0.127
Δ_{1607}	0.047	0.052	0.065†	0.052	0.053	0.048	0.054
Δ_{1658}	−0.199	−0.168	−0.174	−0.151†	−0.198	−0.177	−0.176

Calculated values were obtained using the B3LYP/6-311G* level of theory. Values that are more than 20% different from the calculated values are labeled with a †.

respective spectrum. The spectra in Figure 5 show the accuracy of the minimization algorithm, where we were able to simulate the relative intensities of the 10 modes under consideration for each experimental spectrum. The values used for the simulated spectra in Figure 5 are listed in Table 1. The top row indicates the particular spectrum in the experimental data set that is being modeled. Both the calculated and optimized parameters are shown for each mode corresponding to the six spectra shown.

The results indicate that the large fluctuations in relative intensities observed experimentally may be reproduced theoretically assuming small fluctuations in excited-state properties. In particular, these large changes were reproduced assuming small changes (usually <20%) in the dimensionless deltas. These changes are reasonable as they reflect changes in the excited-state bond lengths of a picometer or less. These changes are averaged out in ensemble measurements but become important in single-molecule observations. This implies that quantitative analysis of the relative intensities of single-molecule experiments is difficult at best. By summing all of the single-molecule spectra obtained in Figure 1A, we obtain a spectrum, shown in Figure 6, that resembles the ensemble spectrum in both SERS and TERS experiments in which the relative intensities across the spectrum are roughly similar.[5,31]

4. CONCLUSIONS

We have determined an explanation of the large relative intensity fluctuations present in single-molecule TERS spectra. In principle these conclusions should also be generalizable to other experiments such as single-molecule SERS; however, that data must still be examined. Based on an analysis of several of the observable Raman peaks, no correlation is seen with respect to peak area or spectral position. The 2D correlation analysis confirms that the fluctuations observed are completely independent. Theoretical calculations and further experiments have ruled out orientation and field gradient as the cause of these effects. Matching of the theoretical spectra to the experimentally obtained fluctuations was achieved by allowing for small variations (<20%) in the lifetime, energy, and geometry of the excited state. The ability to invert experimental measurements to obtain molecular properties of the excited state of the molecule can provide detailed information on the interactions between adsorbates and the surface.

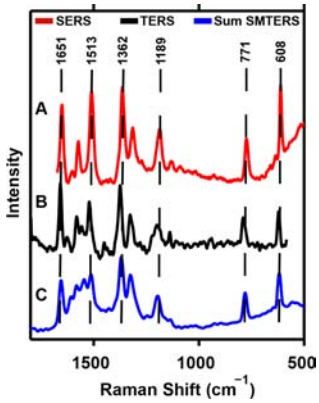

Figure 6. Plot of ensemble (A) SERS and (B) TERS and (C) sum of the single-molecule TERS spectra shown in Figure 1A. The summed SMTERS spectra is compared to ensemble SERS and TERS measurements of R6G. Only spectra with signal above the noise were summed together. In all cases, the areas of the vibrational modes are similar and remain roughly same over time.

■ ASSOCIATED CONTENT

Supporting Information

Complete reference 22. This material is available free of charge via the Internet at http://pubs.acs.org.

■ AUTHOR INFORMATION

Corresponding Author

vanduyne@northwestern.edu

Notes

The authors declare no competing financial interest.

■ ACKNOWLEDGMENTS

This research was made possible by the NSF Center for Chemical Innovation Chemistry at the Space-Time Limit (CHE-082913) and the Department of Energy Basic Energy Sciences SISGR (DE-FG02-09ER16109). Additional support was provided by the National Science Foundation through the following grants (CHE-1152547, CHE-0955689, and DMR-1121262). T.S. is grateful to the National Science Foundation (grant no. CHE-1012207/001) for support.

■ REFERENCES

(1) Nie, S.; Emory, S. R. *Science* **1997**, *275*, 1102.

(2) Kneipp, K.; Wang, Y.; Kneipp, H.; Perelman, L. T.; Itzkan, I.; Dasari, R. R.; Feld, M. S. *Phys. Rev. Lett.* **1997**, *78*, 1667.
(3) Weiss, A.; Haran, G. *J. Phys. Chem. B* **2001**, *105*, 12348.
(4) Neacsu, C. C.; Dreyer, J.; Behr, N.; Raschke, M. B. *Phys. Rev. B: Condens. Matter Mater. Phys.* **2006**, *73*, 193406/1.
(5) Sonntag, M. D.; Klingsporn, J. M.; Garibay, L. K.; Roberts, J. M.; Dieringer, J. A.; Seideman, T.; Scheidt, K. A.; Jensen, L.; Schatz, G. C.; Van Duyne, R. P. *J. Phys. Chem. C* **2012**, *116*, 478.
(6) Steidtner, J.; Pettinger, B. *Phys. Rev. Lett.* **2008**, *100*, 236101/1.
(7) Zhang, R.; Zhang, Y.; Dong, Z. C.; Jiang, S.; Zhang, C.; Chen, L. G.; Zhang, L.; Liao, Y.; Aizpurua, J.; Luo, Y.; Yang, J. L.; Hou, J. G. *Nature* **2013**, *498*, 82.
(8) Zhang, W.; Yeo, B. S.; Schmid, T.; Zenobi, R. *J. Phys. Chem. C* **2007**, *111*, 1733.
(9) Emory, S. R.; Jensen, R. A.; Wenda, T.; Han, M.; Nie, S. *Faraday Discuss.* **2006**, *132*, 249.
(10) Futamata, M.; Maruyama, Y.; Ishikawa, M. *J. Phys. Chem. B* **2004**, *108*, 13119.
(11) Futamata, M.; Maruyama, Y.; Ishikawa, M. *Vib. Spectrosc.* **2004**, *35*, 121.
(12) Haran, G. *Acc. Chem. Res.* **2010**, *43*, 1135.
(13) Maher, R. C.; Dalley, M.; Le, R. E. C.; Cohen, L. F.; Etchegoin, P. G.; Hartigan, H.; Brown, R. J. C.; Milton, M. J. T. *J. Chem. Phys.* **2004**, *121*, 8901.
(14) Dieringer, J. A.; Lettan, R. B., II; Scheidt, K. A.; Van Duyne, R. P. *J. Am. Chem. Soc.* **2007**, *129*, 16249.
(15) Michaels, A. M.; Jiang, J.; Brus, L. *J. Phys. Chem. B* **2000**, *104*, 11965.
(16) Etchegoin, P. G.; Meyer, M.; Blackie, E.; Le Ru, E. C. *Anal. Chem.* **2007**, *79*, 8411.
(17) Etchegoin, P. G.; Meyer, M.; Le Ru, E. C. *Phys. Chem. Chem. Phys.* **2007**, *9*, 3006.
(18) Domke, K. F.; Zhang, D.; Pettinger, B. *J. Phys. Chem. C* **2007**, *111*, 8611.
(19) Pettinger, B.; Ren, B.; Picardi, G.; Schuster, R.; Ertl, G. *J. Raman Spectrosc.* **2005**, *36*, 541.
(20) Zhang, D.; Xie, Y.; Deb, S. K.; Davison, V. J.; Ben-Amotz, D. *Anal. Chem.* **2005**, *77*, 3563.
(21) Silverstein, D. W.; Jensen, L. *J. Chem. Phys.* **2012**, *136*, 064111/1.
(22) Bylaska, E. J., et al. *NWChem, A Computational Chemistry Package for Parallel Computers*, version 5.1; Pacific Northwest National Laboratory: Richland, Washington, 2007 (a modified version).
(23) Nelder, J. A.; Mead, R. *Honeywell Comput. J.* **1965**, *7*, 308.
(24) Noda, I.; Ozaki, Y. *Two-Dimensional Correlation Spectroscopy: Applications in Vibrational and Optical Spectroscopy*; John Wiley and Sons, Ltd.: Chichester, West Sussex, 2004.
(25) Moore, A. A.; Jacobson, M. L.; Belabas, N.; Rowlen, K. L.; Jonas, D. M. *J. Am. Chem. Soc.* **2005**, *127*, 7292.
(26) Banik, M.; El-Khoury, P. Z.; Nag, A.; Rodriguez-Perez, A.; Guarrottxena, N.; Bazan, G. C.; Apkarian, V. A. *ACS Nano* **2012**, *6*, 10343.
(27) Le Ru, E. C.; Etchegoin, P. G. *SERS enhancement factors and related topics*; Elsevier: Amsterdam, 2009.
(28) Banik, M.; Apkarian, V. A.; Park, T. H.; Galperin, M. *J. Phys. Chem. Lett.* **2013**, *4*, 88.
(29) Hennessy, M. H.; Kelley, A. M. *Phys. Chem. Chem. Phys.* **2004**, *6*, 1085.
(30) Shorr, E.; Myers Kelley, A. *Phys. Chem. Chem. Phys.* **2007**, *9*, 4785.
(31) Hildebrandt, P.; Stockburger, M. *J. Phys. Chem.* **1984**, *88*, 5935.